Low-Authority Control of Large Space Structures by Using a Tendon Control System

Y. Murotsu, H. Okubo, and F. Terui
University of Osaka Prefecture, Osaka, Japan

This paper deals with the problem of controlling the vibrations of large space structures by the use of a newly conceived torque actuation device, i.e., a tendon control system. It consists of a pair of tension cables transmitting a control torque to the structure at the moment arm position. The purpose of the study is twofold: first, to establish the analytical framework for low-authority control synthesis; second, to validate the proposed concept through a hardware experiment. A nonlinear optimization approach is proposed for the design of the control gains and the moment arm placement. This approach is useful when the total number of control devices is smaller than the number of critical vibrational modes, and exact pole placement is not possible. A hardware experiment has been done successfully, which shows the fundamental feasibility of the active tendon control for a highly flexible beam. However, for its practical application, further studies are needed, especially on the interactions between the dynamics of the tension cables and the flexible structure.

Introduction

THE use of active feedback forces to control large space structures (LSS) has been studied intensively most recently, and a variety of approaches to the control system design have been proposed.[1,2] Hardware demonstrations using laboratory models (e.g., beam, plate, grid, etc.) also have been performed in many industries, institutes, and universities.[3-6] Most of these studies are based on the use of inertial reaction actuators such as thrusters and momentum wheels. They are external force-producing devices designed with the objective of attitude control. However, these conventional actuators may not best meet the new class of control objectives, e.g., vibration suppression and shape determination of highly flexible structures. For instance, structures may be too weak to allow the attachment of a massive conventional-type actuator. Therefore, actuators of different types (e.g., proof-mass, piezoelectric, environmental) should be developed to meet the objectives.

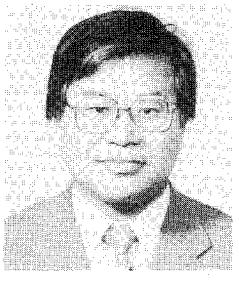

Yoshisada Murotsu was born in Japan in March 1940. He received B.S. and M.S. degrees in aeronautical engineering in 1963 and 1965, respectively, and a doctorate in mechanical engineering in 1969, all from the University of Osaka Prefecture, Sakai, Japan. Since 1968, he has been with the College of Engineering, University of Osaka Prefecture, where he was promoted to Associate Professor of Naval Architecture in 1970, and Chair Professor of Aeronautical Engineering in 1982. From August 1971 to July 1972, Dr. Murotsu was a visiting Research Associate at the University of California, Berkeley. His research activities have included papers on optimum design of automatic flight control systems, systems analysis and planning of transport systems, reliability analysis and optimum design of structural systems, and dynamics and control of large flexible space structures. He is a co-author of *Application of Structural Systems Reliability Theory*, published by Springer-Verlag, as well as several other books. Dr. Murotsu is a Member of the AIAA.

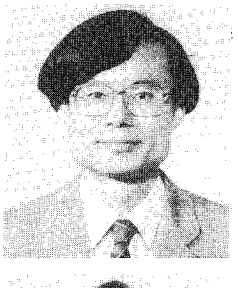

Hiroshi Okubo was born in 1948. He received B.S. and M.S. degrees from Kyoto University in 1971 and 1973, respectively. He also received a doctorate in aeronautical engineering from Kyoto University. Dr. Okubo has been engaged in research in the fields of system identification, state estimation, and optimal control theory and aerospace applications. He also has worked on unsteady aerodynamics of a wing, aircraft gust response, and gust alleviation control problems. Currently, his major areas of research are the identification and control of large flexible space structures and the application of adaptive filtering theory to the diagnosis of sensor/actuator failures. He is a member of the Japan Society for Aeronautical and Space Scientists (JSASS), the Society of Instrument and Control Engineers (SICE), the Institute of Systems, Control, and Information Engineers, the Japan Society of Mechanical Engineers (JSME), and the AIAA.

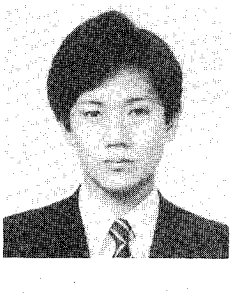

Mr. Terui was born in Japan in 1960. He received B.S. and M.S. degrees in aeronautical engineering in 1984 and 1986, respectively, from the University of Osaka Prefecture, Sakai, Osaka, Japan. Since 1984, he has been a graduate student of the Department of Aeronautical Engineering and is now a Ph.D. candidate. His major subject of research is the control of large flexible space structures.

Presented as Paper 87-2249 at the AIAA Guidance, Navigation, and Control Conference, Monterey, CA, Aug. 17-19, 1987; received Sept. 23, 1987; revision received Jan. 4, 1988.

The authors have proposed a new approach as an alternative, i.e., tendon control of flexible space structures. This is a biomechanical scheme used in nature to control animal motion and configuration, namely, active control of muscles and tendons.[7,8] This concept can be exploited in a man-made flexible structure by the use of force actuators and tension cables. If the activating forces are interstructural, which is called "stiffness control of structures," the time-dependent tensile forces will come into play and add to the complexity of the problems.[9] However, the approach proposed here differs somewhat from such an interstructural control and makes use of transmitting a control torque from the rigid main body to a flexible element. A kind of tendon control system already has been investigated in relevant fields within civil engineering.[10]

Figure 1 is an illustration giving the idea of a tendon control system for suppressing beam vibrations. A pair of actuators at the beam root activates the tendons (i.e., tension cables) to rotate a pair of moment arms attached at a proper position of the structure. Thereby, the beam motion is actively controlled by using the feedback signals from the sensing devices located on the beam.

The use of tendon control provides many advantages for structural control. It is suited to this control task not only because the hardware is simple to implement, but also because a robust colocated control can be realized by using "noncolocated" sensors and actuators. That is, the designer can place the point of control action at any proper location of the flexible appendage or deployable mast, and simultaneously place a massive control actuator at the spacecraft bus.

This paper demonstrates the capability of the tendon control system in low-authority control (LAC) of structures, where the controller is designed by using simple output feedback to increase the effective damping of the critical vibrational modes. The closed-loop system is shown to be stable if an angular rate sensor is located at the moment arm. Then an approach for determining the optimal feedback gains and the optimal arm location is proposed. The result of experimental research using a hardware model is also given.

Tendon Control of a Beamlike Space Structure

System Equations

Many large space structures, although complex, often can be approximated as a more simple structure, such as a beam, plate, or thin shell. That is, the dynamic behavior of these structures may be described approximately by proper beam, plate, or shell equations. For example, a beamlike truss structure with uniform elements may be approximated by a single beam with equivalent stiffness and mass density, as illustrated in Figs. 2a and 2b. When the equivalent beam possesses a large transverse shear rigidity, then the governing equation of motion reduces to Euler-Bernoulli beam equations:

$$\overline{\rho A}\frac{\partial^2 y(x,t)}{\partial t^2}+\overline{EI}\frac{\partial^4 y(x,t)}{\partial x^4}-\frac{\partial}{\partial x}\left[S(x)\frac{\partial y(x,t)}{\partial x}\right]=F_c(x,t) \qquad (1)$$

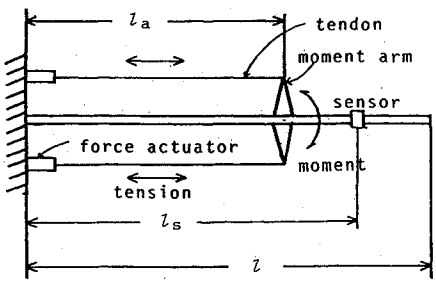

Fig. 1 Tendon control system for beam vibration suppression.

$$F_c(x,t)=-\frac{\partial M_c(x,t)}{\partial x} \qquad (2)$$

where $y(x,t)$ represents instantaneous displacements of the beam from its equilibrium position, and $F_c(x,t)$ and $M_c(x,t)$ are the applied control force and moment distributions, respectively. $S(x)$ denotes the axial tensile force applied to the beam and is assumed to be small and constant. The boundary conditions for a cantilever beam are

$$y(0,t)=\left.\frac{\partial y(x,t)}{\partial x}\right|_{x=0}=0$$

$$\left.\frac{\partial^2 y(x,t)}{\partial x^2}\right|_{x=l}=\left.\frac{\partial^3 y(x,t)}{\partial x^3}\right|_{x=l}=0 \qquad (3)$$

The displacement $y(x,t)$ can be represented by a linear combination of space-dependent eigenfunctions, $Y_n(x)$, multiplied by time-dependent generalized coordinates, $H_n(t)$.

$$y(x,t)=\sum_{n=1}^{\infty} Y_n(x)H_n(t) \qquad (4)$$

Introducing Eq. (4) into Eq. (1) and applying orthogonality conditions of eigenfunctions, one can derive the mode equations for the generalized coordinates

$$\frac{d^2H_n(t)}{dt^2}+\omega_n^2 H_n(t)=Q_n(t), \quad n=1,2,\ldots,\ \omega_1<\omega_2<\cdots \qquad (5)$$

where

$$Q_n(t)=(1/\overline{\rho A}l)\int_0^l F(x,t)Y_n(x)\,dx, \quad n=1,2,\ldots \qquad (6)$$

are generalized modal control forces.

Here we consider the active tendon control of a beamlike structure (see Fig. 1). The objective of LAC synthesis using the tendon torque actuator and output feedback is addressed here. The tendon actuator consists of two force actuators linked with a pair of moment arms through tensile wires and generates control torques at the arm point. Motion along the beam (angular or translational position and rate) is measured using appropriately placed sensors, and the sensor signals are fed back to activate the tension wires. Selection of the sensing devices (i.e., linear or angular sensors) and their placement represents a substantial degree of freedom to the designer and is usually not a straightforward task. In the following, we analyze the stability of the output feedback system and then propose an approach to determine optimum sensor placement and optimum feedback gains.

Stability of the Closed-Loop System

It is widely recognized that velocity feedback control using colocated sensors, i.e., direct velocity feedback (DVFB), is energy dissipative and assures closed-loop stability for an infinite number of modes.[11] However, in engineering practice, the number of modes that excite with the active controller is finite. Hence, the system still may be stable when noncolocated velocity and position feedback are introduced. Here we discuss the stability of the closed-loop system when a finite number of modes are taken into consideration and derive the constraints for gain determination and sensor/actuator placement. Moreover, it is shown that the stability of the system depends not only on the placement of the control devices but also on their type.

Here, we consider output feedback control using one moment arm and a pair of angular displacement and angular rate (velocity) sensors for feedback. Then the control moment $M_c(x,t)$ and generalized force $Q_n(t)$ are given by

$$M_c(x,t)=-\left[K_1\frac{\partial y(l_s,t)}{\partial x}+K_2\frac{\partial}{\partial t}\frac{\partial y(l_s,t)}{\partial x}\right]\delta(x-l_a) \qquad (7)$$

$$Q_n(t) = -[Y_n'(l_a)/\overline{\rho A}l] \sum_{m=1}^{\infty} Y_m'(l_s)[K_1 H_m(t) + K_2 \dot{H}_m(t)] \quad (8)$$

where the prime denotes the derivative with respect to x; K_1 and K_2 are feedback gains; l_a and l_s are actuator and sensor positions, respectively; and $\delta(x)$ denotes a Dirac delta function.

Let us substitute Eq. (8) into Eq. (5) and take the Laplace transform, ignoring initial conditions, to obtain

$$(s^2 + \omega_n^2)H_n(s) = -\frac{1}{\overline{\rho A}l} Y_n'(l_a)(K_1 + K_2 s) \sum_{m=1}^{\infty} Y_m'(l_s)\bar{H}_m(s), \quad n = 1,2,\ldots \quad (9)$$

Then, multiplying both sides of the equation by $Y_n'(l_s)/(s^2 + \omega_n^2)$ and taking summation for $n = 1,2,\ldots$, one obtains the following relation:

$$\sum_{n=1}^{\infty} Y_n'(l_s)H_n(s) = -\frac{1}{\overline{\rho A}l} \sum_{n=1}^{\infty} Y_n'(l_s)Y_n'(l_a)\frac{K_1 + K_2 s}{s^2 + \omega_n^2} \sum_{m=1}^{\infty} Y_m'(l_s)H_m(s) \quad (10)$$

Thus, the characteristic equation of the closed-loop system can be written as

$$1 + \frac{1}{\overline{\rho A}l} \sum_{n=1}^{\infty} Y_n'(l_s)Y_n'(l_a)\frac{K_1 + K_2 s}{s^2 + \omega_n^2} = 0 \quad (11)$$

or

$$\prod_{n=1}^{\infty} (s^2 + \omega_n^2) + (K_1 + K_2 s) \sum_{n=1}^{\infty} B_n \prod_{m \neq n}^{\infty} (s^2 + \omega_m^2) = 0 \quad (12)$$

where

$$B_n = (1/\overline{\rho A}l)Y_n'(l_s)Y_n'(l_a)$$

If one takes the expansion terms to the Nth mode, the characteristic equation can be written in the following form:

$$P^N(s) = s^{2N} + D_{2N-1}s^{2N-1} + \cdots + D_1 s + D_0 = 0 \quad (13)$$

where

$$D_0 = \left(\prod_{n=1}^{N} \omega_n^2\right)\left[1 + K_1 \sum_{n=1}^{N} (B_n/\omega_n^2)\right]$$

$$D_1 = K_2\left(\prod_{n=1}^{N} \omega_n^2\right) \sum_{n=1}^{N} (B_n/\omega_n^2)$$

$$D_{2k} = \left(\prod_{n=1}^{N} \omega_n^2\right) \sum_{j=1}^{N} \sum_{j_2 > j_1}^{N} \cdots \sum_{j_k > j_{k-1}}^{N} \left[1 + K_1 \sum_{n=1}^{N} (B_n/\omega_n^2)\right] \Big/ (\omega_{j_1}^2 \omega_{j_2}^2 \cdots \omega_{j_k}^2)$$

$$D_{2k+1} = K_2\left(\prod_{n=1}^{N} \omega_n^2\right) \sum_{j_1=1}^{N} \sum_{j_2 > j_1}^{N} \cdots \sum_{j_k > j_{k-1}}^{N} 1/(\omega_{j_1}^2 \omega_{j_2}^2 \cdots \omega_{j_k}^2), \quad k = 1,2,\cdots,N-1$$

The following stability result is obtained.

Theorem 1: The closed-loop system with output feedback is stable for the N-mode system, i.e., Eq. (13), if

$$B_n > 0, \quad n = 1,2,\ldots,N \quad (14)$$

$$K_1 > -1 \Big/ \left(\sum_{n=1}^{N} B_n/\omega_n^2\right), \quad K_2 > 0 \quad (15)$$

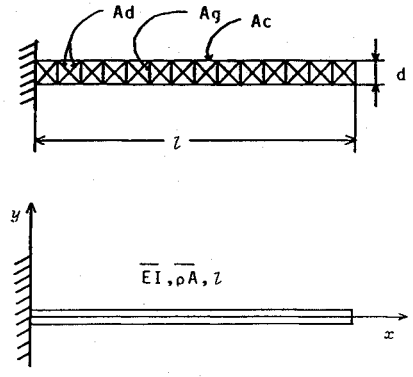

Fig. 2 Cantilever truss structure and equivalent beam with uniform mass distribution.

Proof: Let the odd- and even-order terms of the characteristic polynominal $P^N(s)$ be denoted as $P_0^N(s)$ and $P_e^N(s)$, respectively

$$P^N(s) = P_e^N(s^2) + sP_0^N(s^2) \quad (16)$$

where

$$P_e^N(x) = \left\{\prod_{n=1}^{N} (x + \omega_n^2)\right\}\left[1 + K_1 \sum_{n=1}^{N} B_n/(x + \omega_n^2)\right] = \prod_{n=1}^{N} (x + \omega_n^2) + (K_1/K_2)P_0^N(x) \quad (17)$$

$$P_0^N(x) = K_2\left\{\prod_{n=1}^{N} (x + \omega_n^2)\right\} \sum_{n=1}^{N} B_n/(x + \omega_n^2) \quad (18)$$

The Nth-order polynominal P^N has zeros with strictly negative real parts if, and only if, the zeros of $P_e^N(x)$ and those of $P_0^N(x)$ appear alternately on the real axis and $D_0 > 0$, $D_1 > 0$ (Mikhailov's Theorem).[12] One can easily show that, if conditions (14) and (15) are satisfied, then $D_0 = P_e^N(0) > 0$ and $D_1 = P_0^N(0) > 0$. Since $P_0^N(-\omega_k^2)P_0^N(-\omega_{k+1}^2) < 0$ $(k = 1,2,\ldots, N-1)$ and $P_0^N(-\omega_1^2) > 0$, the kth zero of $P_0^N(x)$, X_k^0, appears between $-\omega_k^2$ and $-\omega_{k+1}^2$. Therefore, the kth zero of $P_e^N(x)$, X_k^e, lies between X_{k-1}^0 and X_k^0 because

$$P_e^N(x_k^0)P_e^N(x_{k+1}^0) = \prod_{n=1}^{N} (x_k^0 + \omega_n^2) \prod_{n=1}^{N} (x_{k+1}^0 + \omega_n^2) = \left[\prod_{n \neq k+1}^{N} (x_k^0 + \omega_n^2)(x_{k+1}^0 + \omega_n^2)\right] \times (x_k^0 + \omega_{k+1}^2)(x_{k+1}^0 + \omega_{k+1}^2) < 0 \quad (19)$$

and

$$P_e^N(x_1^0) = \prod_{n=1}^{N} (x_1^0 + \omega_n^2) < 0 \quad (20)$$

(Q.E.D.)

The condition of Theorem 1 for K_1 is derived from $D_0 > 0$, and it implies that a negative K_1 may be used for the N-mode system. However, when $N \to \infty$, this condition reduces to $K_1 > 0$ and, whenever a rigid-body mode exists (i.e., $\omega_n = 0$), the use of a positive K_1 is requisite.

Since B_n is proportional to the product of mode shapes, the positivity of B_n $(n = 1,2,\ldots,N)$ is assured if the actuators and sensors are colocated. Positivity of B_n also depends on the type of sensor and actuator employed. Table 1 shows B_n's for different types of sensors and actuators. It should be noted that, for instance, if linear transverse displacement/velocity sensors are adopted with a torque actuator such as the tendon controller, the positivity of B_n is not assured by colocation.

Optimization of Gains and Moment Arm Placement

In the preceding section, the stability of the output feedback system has been discussed. Now a general approach is developed for determining the optimal feedback gains and placement of the moment arm.

Table 1 Value of the factor B_n

Sensor	Actuator	B_n
Linear disp./veloc.	Thruster	$Y_n(l_s)Y_n(l_a)/\overline{\rho A}$
	Torquer	$Y_n(l_s)Y'_n(l_a)/\overline{\rho A}$
Angular disp./veloc.	Thruster	$Y'_n(l_s)Y_n(l_a)/\overline{\rho A}$
	Torquer	$Y'_n(l_s)Y'_n(l_a)/\overline{\rho A}$

Optimum Design via Nonlinear Programming

A fundamental objective of a structural control system is the placement of the poles associated with the critical vibrational modes. However, with a constant gain output feedback control, exact pole assignment is possible only when the control devices (i.e., sensors and actuators) satisfy the observability and controllability conditions, and their total number exceeds twice the number of controlled modes. If this requirement cannot be satisfied, as usual in LSS control, exact pole placement is not possible. Hence an approximate pole-placement algorithm should be employed to relocate the poles into some prescribed region of the complex plane and to minimize the location errors.

In general, this problem can be solved by using nonlinear optimization techniques, which relocate the closed-loop poles to desired locations in the complex plane as "closely" as possible, as determined by a particular cost function.

Two objective functions are proposed here. First, the total of the square of pole-location errors in the complex plane would be a reasonable candidate for the objective function to be minimized in this approach:

$$J_1 = (K_1,K_2; l_a,l_s) = \sum_{i=1}^{2N} a_i |P_i(K_1,K_2; l_a,l_s) - P_{d_i}|^2 \quad (21a)$$

where

$$a_i = 1/\omega_i^2, \qquad i = 1,2,\ldots,2N \quad (21b)$$

$P_i(K_1,K_2; l_a,l_s)$ and P_{d_i} $(i = 1,2,\ldots,2N)$ are the $2N$ characteristic roots of the closed-loop system and their desired locations, and the associated weightings, a_i $(i = 1,2,\ldots,2N)$, are used to obtain the uniform improvement in each mode.

Another index of performance could be defined considering the desired damping ratios of N critical modes, ζ_{d_j} $(j = 1,2,\ldots,N)$:

$$J_2(K_1,K_2; l_a,l_s) = \sum_{j=1}^{N} a_j [\zeta_j(K_1,K_2; l_a,l_s) - \zeta_{d_j}]^2 \quad (22)$$

where

$$\zeta_j = \frac{|\alpha_j|}{\sqrt{\alpha^2+\beta^2}}, \quad P_j = \alpha_j + i\beta_j, \qquad j = 1,2,\ldots,N$$

and a_j $(j = 1,2,\ldots,N)$ are weighting factors.

Thus, the approximate pole-location problem reduces to the determination of the optimum gains (K_1 and K_2) and control device placements (l_a and l_s), which minimize the objective function as defined earlier. The problem constraints are that $P_i(K_1,K_2; l_a,l_s)$ $(i = 1,2,\ldots,2N)$ satisfy the characteristic equation and the values of the design parameters (i.e., K_1,K_2; l_a, and l_s) are within some prescribed boundary, i.e.,

$$f_c(K_1,K_2; l_a,l_s) = P^N(P_i) = 0, \qquad i = 1,2,\ldots,N \quad (23)$$

$$g_j(K_1,K_2; l_a,l_s) \leqq 0, \qquad j = 1,2,\ldots,n_c \quad (24)$$

The optimization problem with equality and inequality constraints generally can be solved by using the multiplier method.[13] However, straightforward application of this technique to the equality constraint, Eq. (23), is difficult because the characteristic roots P are implicit functions of the design parameters. Hence, the proposed optimization algorithm explicitly solves the updated characteristic equation for the roots to recompute the objective function and its gradients.

Then, the augmented Lagrangian function is defined by

$$L_t(x,\lambda) = J(x) + \sum_{j=1}^{n_c} \frac{1}{2t_j}[\max\{0,\lambda_j + t_j g_j(x)\}^2 - \lambda_j^2] \quad (25)$$

where $\lambda = (\lambda_1,\lambda_2,\ldots,\lambda_n)^T$ and $t = (t_1,t_2,\ldots,t_{n_c})$ are penalty parameters.

In the optimization scheme, the following steps are carried out:

0) Given initial design parameters $x^0 = (K_1^0, K_2^0, l_a^0, l_s^0)$, $0 \leq \lambda^0 \in R^h$, $0 < t \in R^{n_c}$, $\varepsilon > 0$, $k = 0$.

1) Solve the characteristic equation $f_c(x^k \pm \delta x) = 0$ and obtain $2N$ roots, $P_1,P_2,\ldots,P_{2N}$.

2) Compute the objective function $J(x^k \pm \delta x)$ and the augmented Lagrangian function $L_{t^k}(x^k \pm \delta x,\lambda^k)$.

3) Approximate gradients $\partial L_{t^k}/\partial x$ by central differences and improve design parameters iteratively for unconstrained minimization by use of a conjugate gradient method. Repeat steps 1 and 2 for updated design parameters. If optimal x^k is obtained then go to step 4.

4) Update penalty parameters λ^k and t^k according to the ordinary multiplier method. If

$$\max_i |\max\{g_i(x^k), -(\lambda_i^k/t_i^k)\}| \leqq \varepsilon$$

then complete the iteration, otherwise return to step 1 with $k = k + 1$.

Numerical Example

A numerical example is given in this section to illustrate the application of the proposed design procedure. A flexible truss structure deployed from a rigid spacecraft bus is modeled as a cantilever beam with an equivalent bending rigidity $EI = 7.17 \times 10^7$ Nm, mass per unit length $\rho A = 0.875$ kg/m and length $l = 150$ m. (See Ref. 7 for more detailed data.) Axial force is neglected here, i.e., $S(x) = 0$. In Table 2, the mode frequencies are given up to the fourth mode. The modes with higher frequencies are truncated from the dynamic model.

A tendon actuator is mounted to the structure with several angular displacement/velocity sensors at the arm position (i.e., $l_a = l_s = l_c$).

Let the design parameters of this control system be the feedback gains K_1 and K_2, which are the gains for the angular displacement and angular velocity, respectively, at the colocation position l_c.

Numerical analysis of optimization using the two proposed objective functions is described in the following.

Table 2 Natural frequencies of a beamlike truss structure

Mode No.	Frequency ω_n, rad/s
$n = 1$	1.41359
$n = 2$	8.86272
$n = 3$	24.82514
$n = 4$	48.64171

The objective function J_2 is employed to optimize the damping ratios for the critical modes. In the optimization, the desired damping ratios are assumed to be $\zeta_{d_i} = 0.5$ and the weighting factors are set as $a_j = 1$ for all j.

The optimum gains K_1^* and K_2^* are sought for a number of different colocation positions. The resulting optimum objective function $J_2(K_1^*, K_2^*; l_c)$ is plotted in Fig. 3 as a function of l_c. The optimum gains, achieved damping ratios, and pole locations are listed in Table 3 for three colocation positions (i.e., $l_c/l = 0.083$, 0.6, and 1.0), where the objective function exhibits distinct local minima.

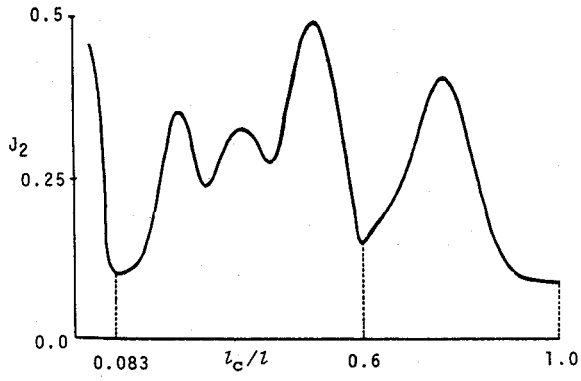

Fig. 3 Variation of minimum objective function as a function of colocation position.

The objective function J_2 is useful as long as the closed-loop poles have complex roots. However, in many cases, when the feedback gains are increased, some of the poles are likely to move to the real axis and the use of a performance index based on damping ratio becomes ineffective.

The use of the objective function J_1 seems to be more reasonable and has a general capability for approximate pole placement. In this example, the placement of the target pole location is determined for providing the same damping ratio, $\zeta_{d_1} = 0.447$, in each mode. The result of gain optimization for the case of colocation position $l_c/l = 1.0$ is summarized in Table 4.

Hardware Experiment

Experimental research has been performed using a hardware model in the laboratory. It is designed to prove the concept proposed, i.e., low-authority control of flexible structures by using a tendon control system. Details of the hardware setup are given in the following.

Experimental Apparatus

A clamped-free homogeneous flexible beam hanging in the vertical direction has been chosen as the test structure. This configuration is a simple, continuous structure with dynamic characteristics that are representative of a variety of flexible elements in many space structures (e.g., booms and antennas).

Table 3 Results of optimization for three different colocation positions

Feedback gains			Modal damping ratios			
K_1	K_2	Optimum J_2	ζ_1	ζ_2	ζ_3	ζ_4
		$l_c/l = 0.083$				
-7.187×10^6	7.704×10^5	0.1026	0.5037	0.3666	0.5393	0.2114
		Pole locations				
		Real part	−0.2414	−2.906	−12.18	−7.946
		Imaginary part	0.4139	7.374	19.02	36.73
		$l_c/l = 0.6$				
-1.178×10^5	6.100×10^5	0.1535	0.5356	0.2047	0.2453	0.4846
		Pole locations				
		Real part	−0.7523	−1.897	−7.391	−17.32
		Imaginary part	1.186	9.068	29.21	31.26
		$l_c/l = 1.0$				
-4.017×10^5	1.731×10^5	0.09147	0.5044	0.4544	0.4965	0.2011
		Pole locations				
		Real part	−0.4284	−4.325	−11.60	−7.952
		Imaginary part	0.7334	8.477	20.29	38.74

Table 4 Optimum gains obtained by using the objective function J_1

Optimum gains			Pole placement			
K_1	K_2	Optimum J_1	P_1	P_2	P_3	P_4
-2.508×10^5	1.677×10^5	0.3011	−0.3165 ±1.113i $\zeta = 0.2735$	−3.617 ±8.913i $\zeta = 0.3760$	−11.15 ±22.03i $\zeta = 0.4515$	−8.463 ±39.07i $\zeta = 0.2117$
			Target pole locations			
		−0.6299 ±1.252i	−3.980 ±7.960i	−10.73 ±21.46i	±21.46i	−21.46 ±42.93i
	$\lvert P_{di} - P_i \rvert / \omega_i$	0.2425	0.1151	0.2851		0.2787

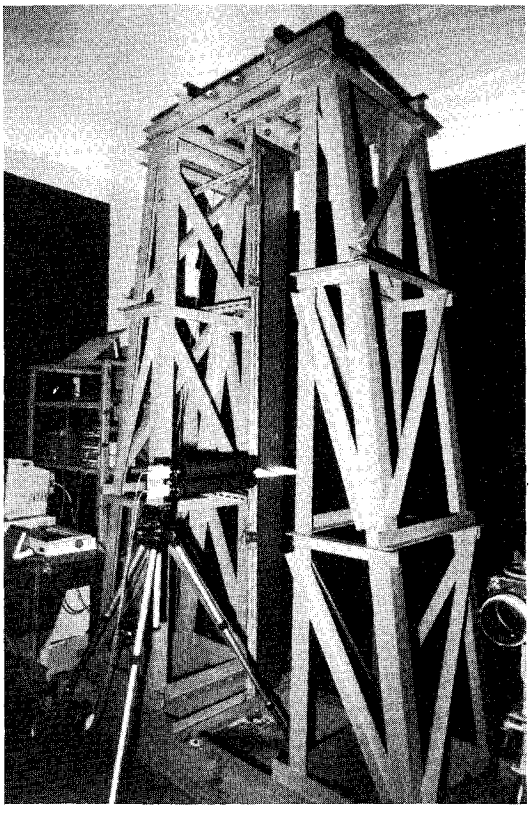

Fig. 4 Experimental apparatus.

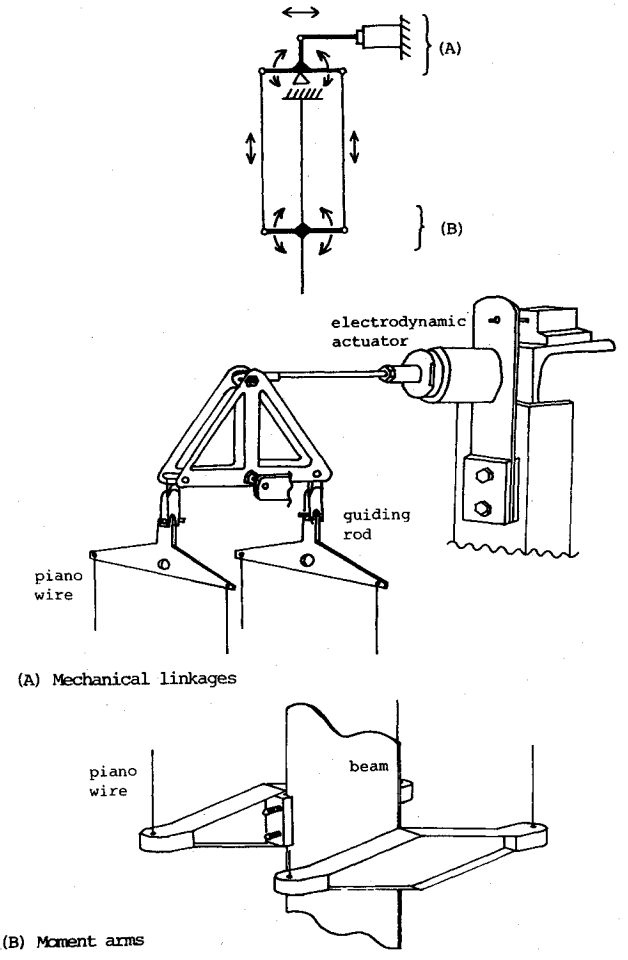

Fig. 5 Configuration of the tendon actuator system.

A photograph of the experimental apparatus (i.e., the flexible beam and its support structure) is shown in Fig. 4. The beam consists of 18-8 stainless steel with a length of 2.4 m. It weighs 2.74 kg and has a cross section of 150×1 mm. (See Table 5.) The support structure (i.e., test stand) is constructed of steel angles and channels and weighs 700 kg in total. The stiffness of the support structure is large enough so that its dynamics do not interact with those of the flexible beam.

The dynamics of the beam motion are modeled by Euler-Bernoulli theory, including loads due to gravitational force, i.e., $S(x) = Ag(1 - x)$. For experimental verification of the dynamic model, analysis for the measured beam responses was performed by means of an impact method. Table 6 presents the theoretically and experimentally determined natural frequencies of the lowest eight modes. The theoretical natural frequencies without gravity are listed in the first column to show that the gravity effect is remarkable, especially at lower frequencies. On the other hand, the gravitational force changes the corresponding mode shapes very little (not shown here).

Configuration of the prototype tendon actuator is shown in Fig. 5. An electrodynamic force actuator and appropriate mechanical link are designed for the purpose of active tendon control. The force actuator consists of a cylindrical electromagnetic coil that is free to move in a permanent magnetic cylinder. It has a capability of applying 4 Newton of force for a maximum 2-A input over about a 70-Hz bandwidth and with nonlinearity of 1% for a displacement range of ± 18 mm.

With the aid of a properly designed mechanical link system, tension cables, and moment arms, the control moment generated by the force actuator can be transmitted almost linearly to the arm position. To allow the beam's response to be free from torsional vibrations, two pairs of arms are attached to both side edges of the beam. Hence, a total of four tension cables are used to link the moment arms to the guiding rods of the mechanical linkage mounted at the beam root. The tension cables are made of piano wires of 0.35 mm in diameter.

An initial tensile force of equal magnitude is applied to each cable by adjusting screw joints. This static loading is useful

Table 5 Characteristics of a beam used for hardware experiment

Material	Stainless steel
Length, m	2.4
Width, mm	150
Thickness, mm	1
Flexual rigidity EI, Nm^2	2.39
Mass density per unit length, $kg\text{-}m^{-1}$	1.14
Weight, kg	2.74

both for preventing the cables from being loose during the control action and for keeping the total axial stress applied to the beam constant, thereby, avoiding problems due to time-varying stiffness. Moreover, it increases resonant frequencies of the cable vibration in the lateral direction.

Figure 6 shows the sensing system used in the control loop. Two sets of electro-optical position sensing devices (PSD) made by Hamamatsu Photonics Corporation are employed. Each PSD unit measures the two-dimensional displacements with a resolution of 0.02% over a 20-mm range and a 0.5-kHz bandwidth. A pair of light emitting diode (LED) targets are attached to the beam at a small distance above and below the arm position. Thereby, the beam deflection angle can be obtained from the displacements of the target pair by taking the divided difference in the plane.

The entire assembly of the control system is shown in Fig. 7. The two-dimensional displacements of the LED targets are transduced into voltage signals and inputted to a 12-bit analog-to-digital converter board mounted on an NEC 9801-VM

microcomputer. This microcomputer chosen for the control function is based on a V30 16-bit microprocessor operating at a 10-MHz clock speed. An 8087 arithmetic processor is also mounted to accelerate the processing speed in floating-point operations. A 12-bit digital-to-analog converter is dedicated to outputting a voltage signal proportional to the commanded control forces. Since the employed actuator drive amplifier has a current feedback loop with compensation networks, the input-to-output relation between the commanded voltage and the realized control force is found to be highly linear in the frequency range of interest. Therefore, the inner loop control using a force sensor, which is shown in Fig. 7, is not required.

Results and Discussion

An output feedback control law was tested by using the prototype tendon actuator and the sensing system. Computer software has been developed to carry out the control task. The deflection angle of the beam at the arm position is computed by using the PSD output signals as described earlier. Since no state estimator is used in the controller, the angular displacements are differentiated numerically to provide the local rate information. A digital filter based on Simpson's rule is used for the numerical differentiation. Angular displacement/velocity thus obtained are multiplied by constant gains to form the actuator command. The real-time control loops are coded directly in assembly language and, thereby, sampling time can be chosen as short as 2 ms.

The open- and closed-loop responses of the beam are shown in Figs. 8 and 9, where the excitation input is a unit impulse to the electrodynamic actuator and the output is the beam displacement at the arm position. The arm location was at 60% beam length from the root, which is one of the best colocation positions when the first four modes are considered in the controller design. This location was selected considering the required maximum control torque and the length of tension wires. In this experiment, noise filters are not fully applied in order to avoid phase delays in the range of high frequencies; therefore, the feedback gain is chosen to be within a very low level determined from noise considerations. Furthermore, no position feedback was introduced.

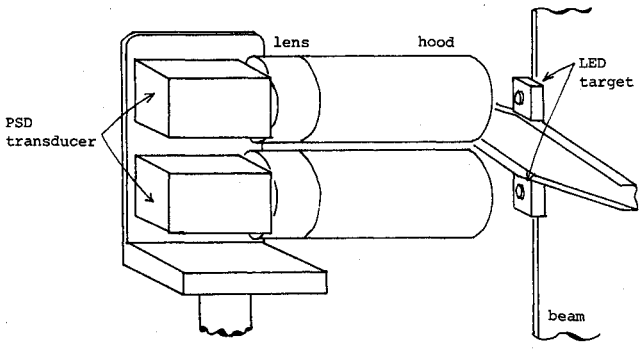

Fig. 6 PSD's and LED targets.

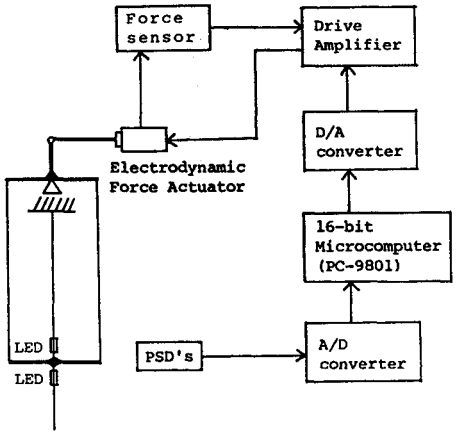

Fig. 7 Block diagram of the controller.

In Fig. 8, many lightly damped modes excited by the moment impulse can be seen. The open-loop modal damping, primarily due to friction of the actuator coil and joints as well as atmospheric drag, is estimated to be about 1.3% of critical damping for the first mode.

The closed-loop response shows that this controller provides an added effective damping to the structure. Although the increase of damping is not remarkable (about 3.3% of critical damping) for the first mode, there is no observable spillover into the higher frequencies for this configuration and gain. Amplitudes of the Fourier spectra are plotted also in Figs. 8 and 9. The decrease in the peak amplitude for the third and higher modes is more remarkable as compared with that for the lowest two modes. This is due to the characteristic of the torque actuation with angular velocity feedback. The first and second modes would be suppressed further if linear velocity feedback were used.

In this preliminary experiment, experimental validation has been achieved for the fundamental feasibility of the tendon control system. There are, however, several problems to be considered for engineering practice. The following points should be studied further: 1) influence of the dynamics of the tendon actuator on beam motion; 2) material of the tension cables should have both high rigidity and low density; 3) design of the magnitude of initial tension considering the effect of axial stress on the dynamics; and 4) implementation of tendons and moment arms in actual space structures.

The first item is very important because when long tendon wires are used in practice, they cannot transmit the control torques immediately to the arm position. In this case, the colocation condition for the sensor/actuator placement is evidently violated, and the transmission delay due to wave traveling in tension cables may cause instability.

This problem was examined with the existing experimental hardware. In order to investigate the closed-loop system stability in the range of high frequencies, the bandwidth of the actuator dynamics was increased (by reducing the frictional damping in the rotational motion of the linkage). A typical result for this revised model is shown in Fig. 10. When the gain was increased, severe interactions between the vibrating wires and the beam caused instability. Further studies are required to investigate this phenomenon of instability and to develop the procedure for designing a refined controller that alleviates the unstable interaction. The results and discussion for further experiments are given in Ref. 14.

Closed-loop response of the improved control system is shown in Fig. 11[14] to demonstrate that the new design is effective in avoiding the instability due to structural/controls interaction. The figure illustrates the free-vibration decay with the feedback circuit switched on and demonstrates the increase in effective damping by feedback. There is no observable high-

Table 6 Natural frequencies for beam (Hz)

	Euler-Bernoulli theory		Timoshenko	
Modes	without g	with g	with g	Experiment
1	0.14	0.42	0.42	0.42
2	0.88	1.28	1.28	1.28
3	2.42	2.90	2.90	2.92
4	4.74	5.26	5.26	5.35
5	7.83	8.39	8.39	8.55
6	11.70	12.29	12.28	12.45
7	16.34	16.93	16.93	17.33
8	21.76	22.35	22.36	22.85

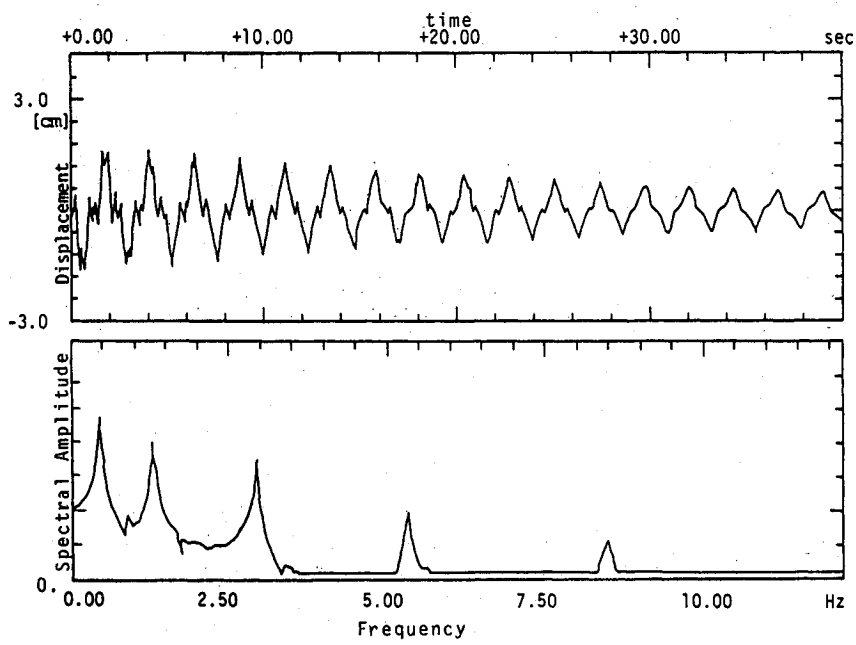

Fig. 8 Free-impulse response of the beam motion at the arm position.

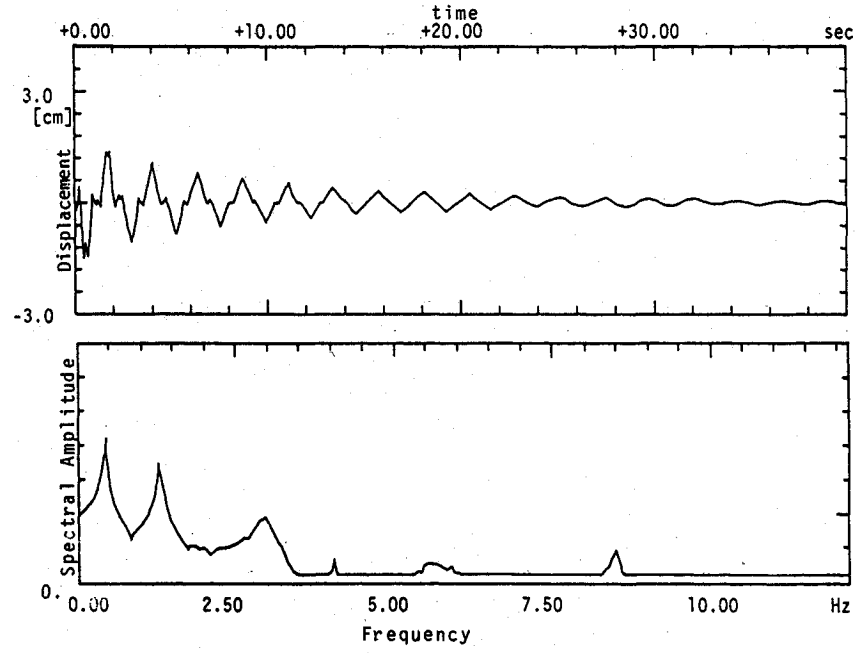

Fig. 9 Closed-loop response for DVFB control using rate measurements at the moment arm.

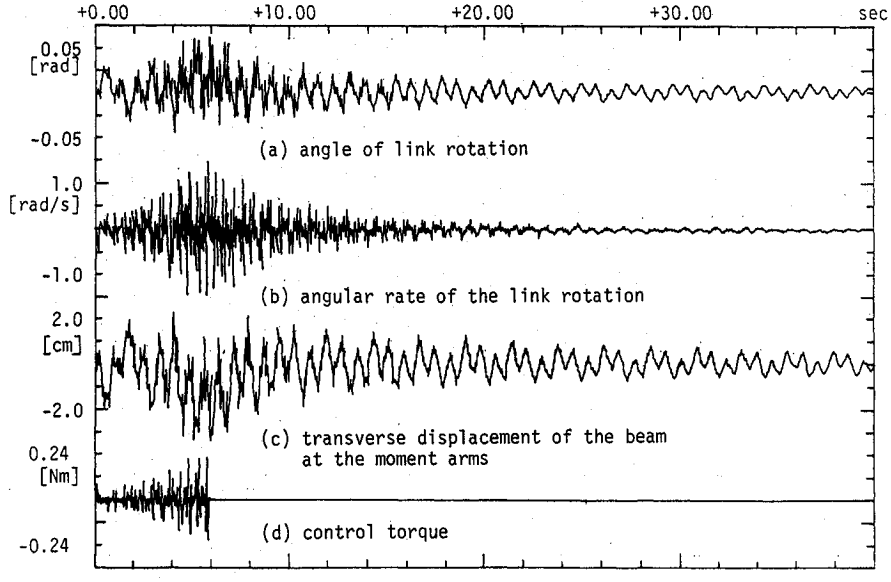

Fig. 10 Typical trace of the closed-loop system instability.

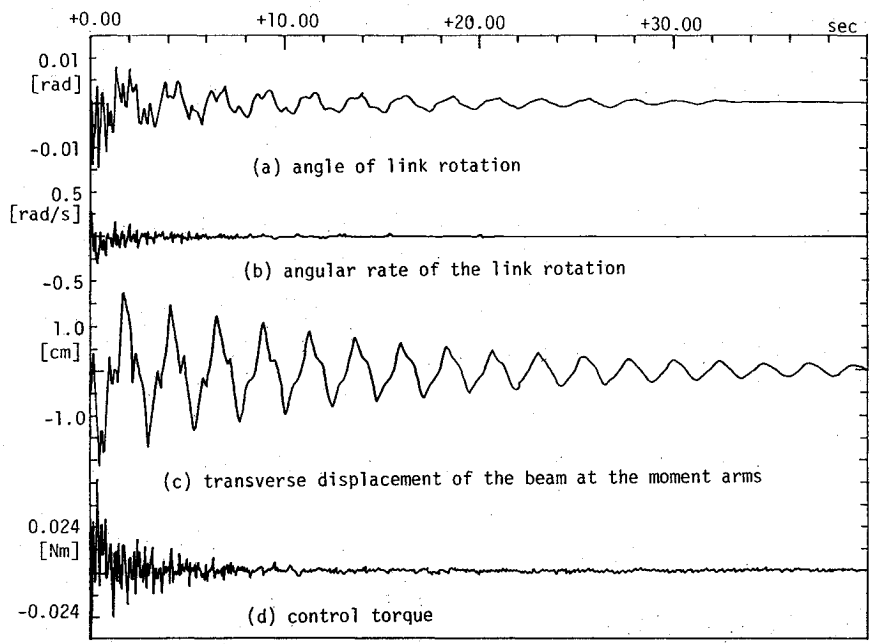

Fig. 11 Closed-loop response for the strict colocation control using a rate sensor mounted at the mechanical link.

frequency modes uncontrolled. The new controller differs from the former unstable one in that it uses feedback of the angular velocity of the mechanical link mounted at the beam root and activated directly by the electrodynamic motor. Thereby, this controller yields a promised stability owing to the strict "colocation" of the sensor/actuator pair.

With these experimental results, strict colocation of the sensor/actuator (i.e., placement of the rate sensor at the mechanical link) is recommended for the actual implementation of a low-authority controller. However, the analysis developed in the preceding sections (with the assumption of virtual colocation condition) is still useful for the purpose of initial design. In a more advanced design strategy, the controller should be based on a two-level control architecture known as low-authority control (LAC)/high-authority control (HAC). The HAC is designed so that the controller performs a given mission optimally using a state observer and modal state feedbacks. Thus, further studies are needed for precise modeling of the dynamics of the tendon actuator and developing an efficient controller for the interacted tendon/structure system.

Conclusions

A newly conceived tendon control concept is given for space structure vibration suppression. The analytical framework has been established for the design and gain synthesis of low-authority controllers using tendon actuator and output feedbacks. The design method proposed is based on a nonlinear optimization scheme in which the feedback gains and control device placements are determined to minimize the aggregated errors in the modal dampings or pole locations.

A hardware experiment has been performed to validate the feasibility of the tendon control system for a beam structure. This experiment has been successful in that the prototype system achieved good vibration suppression in the case of a proper damping applied to the tendon actuator. It also indicated that further studies are required in the identification and modeling of the dynamics of tendon actuator system. Interactions between the dynamics of the tension cables and flexible beam should be eliminated by a proper design of the control system (e.g., LAC/HAC design taking into account the tendon actuator dynamics).

Acknowledgments

The authors are grateful to Mr. A. Mitsuya for his work on the hardware experiment. A part of this study is financially supported by a Grant-in-Aid for scientific research from the Ministry of Education, Science, and Culture of Japan. All of the computations were carried out by using ACOS-850 at the Computer Center of the University of Osaka Prefecture.

References

[1]Nurre, G. S., Ryan, R. S., Scofield, H. N., and Sims, J. L., "Dynamics and Control of Large Space Structures," *Journal of Guidance, Control, and Dynamics*, Vol. 7, Sept.-Oct. 1984, pp. 514–526.

[2]Aubrun, J. N., Breakwell, J. A., Gupta, N. K., and Lyons, M. G., "ACOSS 12 (Active Control of Space Structures)," Rome Air Development Center, Rept. RADC-TR-84-28, Feb. 1984.

[3]Strunce, R. R. and Turner, J. D., "An Investigation of Enabling Technologies for Large Precision Space Systems," Charles Stark Draper Lab., Cambridge, MA, Rept. CSDL-R-1499, Vol. 4, Nov. 1981.

[4]Meirovitch, L., Baruh, H., Montgomery, R. C., and Williams, J. P., "Nonlinear Natural Control of an Experimental Beam," *Journal of Guidance, Control, and Dynamics*, Vol. 7, July-Aug. 1984, pp. 437–442.

[5]Schaechter, D. B. and Eldred, D. B., "Experimental Demonstration of the Control of Flexible Structures," *Journal of Guidance, Control, and Dynamics*, Vol. 7, Sept.-Oct. 1984, pp. 527–534.

[6]Schaefer, B. E. and Holzach, H., "Experimental Research on Flexible Beam Modal Control," *Journal of Guidance, Control, and Dynamics*, Vol. 8, Sept.-Oct. 1985, pp. 597–604.

[7]Murotsu, Y., Okubo, H., Matsumoto, Y., Okawa, Y., and Terui, F., "Tendon Control System for Flexible Space Structures," *Bulletin of the University of Osaka Prefecture*, Ser. A, Vol. 34, No. 1, 1985, pp. 1–11.

[8]Okubo, H., Murotsu, Y., and Terui, F., "Failure Detection and Identification in the Control of Large Space Structures," *Proceedings of the 10th IFAC World Congress on Automatic Control*, Vol. 6, Pergamon, Oxford, 1987, pp. 172–177.

[9]Fanson, J. L., Chen, J. C., and Caughey, T. K., "Stiffness Control of Large Space Structures," *Workshop on the Application of Distributed Parameter Theory to the Control of Large Space Structures*, Jet Propulsion Lab., June 1982, pp. 351–364.

[10]Roorda, J., "Experiments in Feedback Control of Structures," *Proceedings of the 1st IUTAM Symposium on Structural Control*, North-Holland, Amsterdam, 1979, pp. 629–661.

[11]Balas, M. J., "Direct Velocity Feedback Control of Large Space Structure," *Journal of Guidance, Control, and Dynamics*, Vol. 2, May–June 1979, pp. 252–253.

[12]Yamamoto, M., *Stability Theory of Ordinary Differential Equations*, Jikkyo Suppan, 1979, pp. 181–182.

[13]Powell, M. J. D., *Optimization*, edited by R. Fletcher, Academic, New York, 1969.

[14]Okubo, H., Murotsu, Y., Mitsuya, A., and Terui, F., "Research on Tendon Control System for Flexible Structures," *Modeling and Simulation of Distributed Parameter Systems, Proceedings of the IMACS/IFAC Symposium*, Hiroshima, 1987, pp. 647–654.